Appl. Phys. A 80, 537–540 (2005)
DOI: 10.1007/s00339-004-3049-4

Applied Physics A
Materials Science & Processing

H.W. KIM✉
N.H. KIM

Growth of β-Ga_2O_3 nanobelts on Ir-coated substrates

School of Materials Science and Engineering, Inha University, Incheon 402-751, Republic of Korea

Received: 7 May 2004/Accepted: 20 September 2004
Published online: 3 November 2004 • © Springer-Verlag 2004

ABSTRACT We demonstrate the production of gallium oxide (Ga_2O_3) nanobelts on iridium (Ir)-coated substrates by thermal evaporation of GaN powders. Scanning electron microscopy revealed that the product consisted of nanobelts with widths in the range of 100–700 nm and thicknesses less than 1/5 of the widths. X-ray diffraction and high-resolution transmission electron microscopy indicated that the nanobelts have the single-crystalline monoclinic structure of Ga_2O_3. The photoluminescence spectrum under excitation at 325 nm showed a broad band with a prominent emission peak around 433 nm.

PACS 81.07.-b

1 Introduction

Investigation of one-dimensional (1-D) nanostructures, such as nanowires, nanorods, and nanobelts, is likely to have technological significance for nanoelectronics and optoelectronics due to their novel physical properties [1–4]. Among them, the nanowires [5–10] and the nanobelts [3] of the family of oxides have recently drawn much interest. Since Ga_2O_3 is a stable wide-gap compound with intense luminescence properties [3], researchers have studied the growth of Ga_2O_3 nanowires by various techniques such as dc arc discharge [11, 12] and thermal heating or evaporation [13–19]. Also, some researchers have prepared Ga_2O_3 nanobelts by thermally heating or evaporating Ga_2O_3 powders mixed with active carbon/carbon nanotubes [17] or with graphite [20], GaN powders [21, 22], a mixture of Ga and Ga_2O_3 powders [23], a mixture of Ga and SiO_2 powders [24], and a metallic Ga source [25].

Up to now, although various metals such as Au [26–31], AuPd [32], Ni [33], Fe [34], and Al [35] have been investigated with regard to their catalytic roles in synthesizing 1-D nanostructures of various inorganic materials, to our best knowledge, synthesis of any nanostructure on iridium (Ir) substrates has not been reported to date. Also, even though Ga_2O_3 nanowires have been produced using transition-metal powders [11, 12], Au layers [18], and In layers [19], the preparation of Ga_2O_3 nanobelts on metal layers or using metal catalysts has never been reported. Since Ir is thermally stable and an effective oxidation barrier, we expect that it can be a potential electrode material for future solid-state nanodevices. In this paper, we describe the production of β-Ga_2O_3 nanobelts on Ir layers. We have employed thermal evaporation of GaN powders at a temperature of 900 °C.

✉ Fax: +82-32-860-7544, E-mail: hwkim@inha.ac.kr

2 Experimental

We used thermally grown SiO_2 on Si(001) as a starting material onto which a layer of Ir (about 150 nm) was deposited by radio-frequency magnetron sputtering. The experimental apparatus is shown in Fig. 1. The 99.99%-pure GaN powders and the substrate, respectively, were placed on the lower and the upper holder in the vertical tube furnace. The powder-to-substrate distance was 5 mm. During the experiment, a constant flow of nitrogen (N_2) was maintained at a flow rate of 500 sccm. The temperature near the substrate was about 900 °C for 2 h. After evaporation, the substrate was cooled and subsequently taken out from the furnace for structural and optical characterization. A thin layer of wool-like material was found on the surface of the substrate.

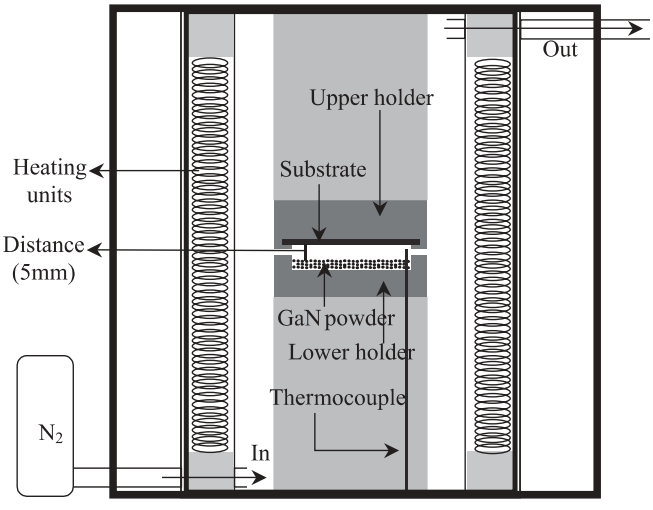

FIGURE 1 Schematic illustration of the apparatus used in this work

The structural properties of the as-grown products were investigated using X-ray diffraction (XRD, X'pert MRD-Philips) with Cu $K\alpha_1$ radiation ($\lambda = 0.154056$ nm), scanning electron microscopy (SEM, Hitachi S-4200), and transmission electron microscopy (TEM, Philips CM-200) with energy-dispersive X-ray spectroscopy (EDS) installed. TEM specimens were prepared by sonicating in acetone, and subsequently dropping onto a holey carbon film supported on a copper grid. Photoluminescence (PL) measurements were carried out at room temperature using a He–Cd (325 nm, 55 mW) laser as the excitation light source.

3 Results and discussion

The XRD pattern shown in Fig. 2 reveals the overall crystal structure of the product on an Ir-coated substrate. Miller indices are indicated on each diffraction peak. The diffraction peaks of (004), ($\bar{1}$04), ($\bar{2}$02), ($\bar{1}$11), (111), ($\bar{1}$13), and ($\bar{2}$13) correspond to the monoclinic β-Ga_2O_3 structure with lattice constants $a = 5.80$ Å, $b = 3.04$ Å, and $c = 12.23$ Å (JCPDS: 11-0370). Additionally, (111) and (200) diffraction peaks of Ir and the (0004) peak of Si (not shown here) from the substrate were detected. It is noteworthy that the (110) diffraction peak of GaIr was also found.

Figure 3a is a typical plan-view SEM image of the deposits on the substrate surface, showing an agglomeration of 1-D nanostructures over a large area. Figure 3b is a SEM image of the side view of the 1-D deposits, revealing random growth directions. Statistical analysis of many SEM images shows that the deposits have widths ranging from 100 to 700 nm, thicknesses less than 1/5 of the widths, and lengths up to several tens of micrometers. Figure 3c is a representative high-magnification SEM image of the deposits, indicating that their geometrical shape is belt-like. The nanobelts have almost uniform widths and smooth surfaces, with no nanoparticles at their tips.

Figure 4a shows the TEM image of the products, revealing the morphology of the belts. The EDS analysis indicated

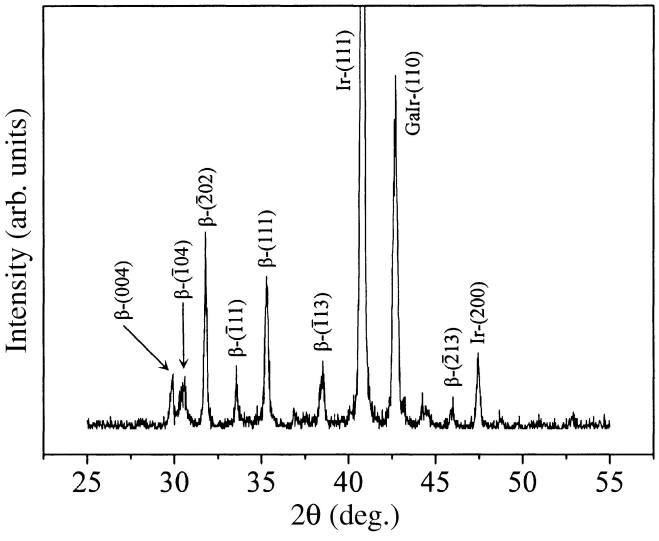

FIGURE 2 XRD pattern recorded from the products on an Ir-coated substrate

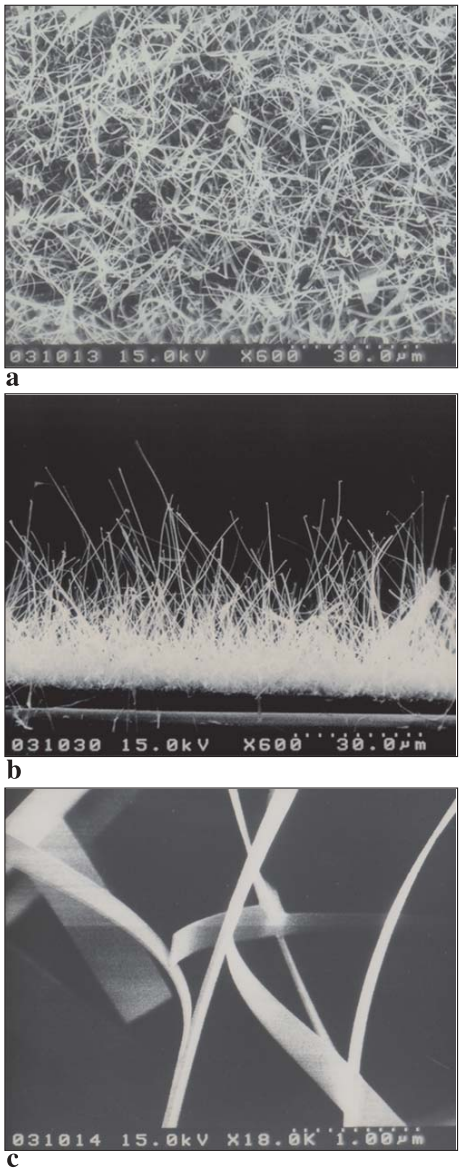

FIGURE 3 (**a**) Plan-view and (**b**) side-view SEM images of the products. (**c**) High-magnification SEM image

that the synthesized nanobelts consist of only Ga and O elements, regardless of the position in the nanobelts from the stem to the ends. The typical EDS spectrum, recorded from a single nanobelt, is shown in Fig. 4b. The C- and Cu-related signals, respectively, are due to the contamination of C while preparing TEM specimens and the presence of Cu grids.

Figure 4c shows the TEM image of a nanobelt and the corresponding selected-area electron diffraction (SAED) pattern, recorded perpendicular to the nanobelt long axis. The SAED pattern can be indexed for the [1$\bar{2}$1] zone axis of crystalline β-Ga_2O_3. The length direction of the nanobelt, indicated by an arrow, is along the [$\bar{1}$01] direction. Figure 4d is a high-resolution TEM (HRTEM) image of the nanobelt shown in Fig. 4c, revealing perfect crystallinity. The interplanar spacings are about 0.28 nm and 0.25 nm, respectively, corresponding to the ($\bar{2}$02) and (111) planes of monoclinic β-Ga_2O_3.

We surmise that the Ga atoms from GaN powders react with O atoms, resulting in the formation of Ga_2O_3 nanobelts.

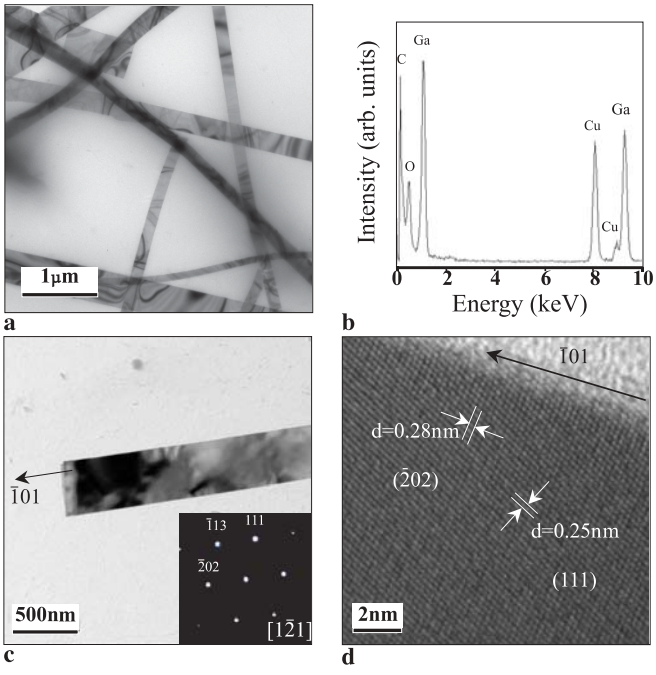

FIGURE 4 (**a**) TEM image of the products. (**b**) EDS spectrum of a single β-Ga_2O_3 nanobelt. (**c**) TEM image of a single β-Ga_2O_3 nanobelt. The *inset* shows the corresponding SAED pattern recorded along the $[1\bar{2}1]$ zone axis. (**d**) HRTEM image

We believe that the oxygen in the Ga_2O_3 has originally come from the air leakage or the residual oxygen in the furnace. When the synthesis was carried out under the same conditions on conventional substrates such as sapphire and bare Si, in the absence of Ir layers, we did not obtain nanobelts. We have produced the belt-like structures on SiO_2 substrates but they were parts of tree-shaped nanostructures. Accordingly, we deduce that the Ir layer affects the formation of Ga_2O_3 nanobelts in this synthesis route. Since SEM images and EDS measurement indicate that all of the nanobelt tips are free of metal nanoparticles, we surmise that the growth of Ga_2O_3 nanobelts in the present route is not dominated by a tip-growth vapor–liquid–solid mechanism. Since the GaIr diffraction peak as well as the Ir diffraction peak was observed, it is likely that some of the Ga generated from the GaN powder reacts with Ir to form the GaIr compound. Therefore, both Ir and GaIr may remain on the substrate surface during the synthesis process. Intensive investigation is required to derive the exact mechanism for the formation of Ga_2O_3 nanobelts in the present work.

The PL spectrum of the deposits at room temperature is shown in Fig. 5. There is an apparent broad, strong PL emission band, which can be a superimposition of several peaks. The blue emission peak at 433 nm is known to be associated with vacancies in Ga_2O_3 [36, 37]. According to Binet and Gourier [38], an electron in a donor is captured by a hole in an acceptor to form a trapped exciton, which recombines radiatively and emits a blue photon. The shoulder peak centered at around 520–550 nm may correspond to a defect level with a different recombination mechanism [39]. Also, we observe the red peak centered at around 700 nm, arising from intrinsic impurities or nitrogen incorporation during the evaporation process under the N_2 gas flow [39]. Although further systematic study is necessary in order to reveal the mechanism of

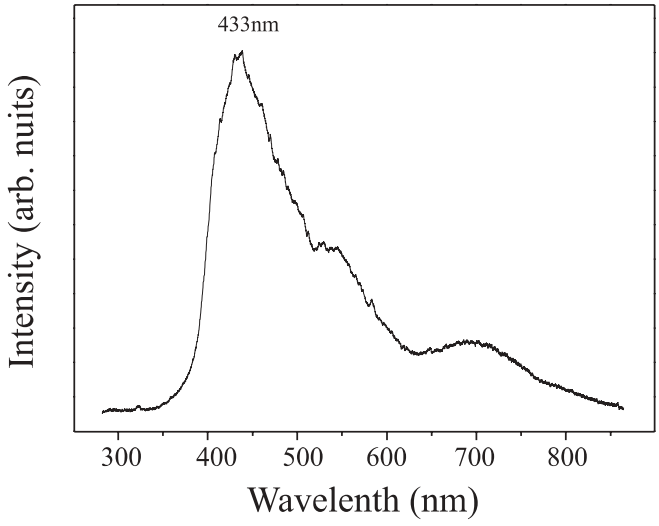

FIGURE 5 Room-temperature PL spectrum of the products with an excitation wavelength of 325 nm

the observed emission, Ga_2O_3 nanobelts may have potential application in optoelectronic nanodevices due to their possibilities of strong emission.

4 Conclusions

In summary, we successfully synthesized single-crystalline monoclinic Ga_2O_3 nanobelts on Ir-coated substrates via a thermal evaporation method of heating GaN powders at 900 °C under N_2 flow. The obtained β-Ga_2O_3 nanobelts, with diameters in the range of 100–700 nm and lengths up to several tens of micrometers, are single crystalline and grew along the $[\bar{1}01]$ direction. The PL spectrum shows a prominent emission peak around 433 nm.

ACKNOWLEDGEMENTS This work was supported by an Inha University research grant (No. INHA-31633).

REFERENCES

1 E.W. Wong, P.E. Sheehan, C.M. Lieber: Science **277**, 1971 (1997)
2 J.T. Hu, T.W. Odom, C.M. Lieber: Acc. Chem. Res. **32**, 435 (1999)
3 Z.W. Pan, Z.R. Dai, Z.L. Wang: Science **291**, 1947 (2001)
4 L.F. Dong, J. Jiao, D.W. Tuggle, J. Petty, S.A. Elliff, M. Coulter: Appl. Phys. Lett. **82**, 1096 (2003)
5 P. Yang, C.M. Lieber: Science **273**, 1836 (1996)
6 Z.L. Wang, R.P. Gao, J.L. Gole, J.D. Stout: Adv. Mater. **12**, 1938 (2000)
7 C.H. Liang, G.W. Meng, Y. Lei, F. Phillipp, L.D. Zhang: Adv. Mater. **13**, 1330 (2001)
8 Z.G. Bai, D.P. Yu, H.Z. Zhang, Y. Ding, X.Z. Gai, Q.L. Hang, G.C. Xiong, S.Q. Feng: Chem. Phys. Lett. **303**, 311 (1999)
9 M.H. Huang, Y. Wu, H. Feick, N. Tran, E. Weber, P. Yang: Adv. Mater. **13**, 113 (2001)
10 Y.Z. Zin, Y.Q. Zhu, K. Brigatti, H.W. Kroto, D.R.M. Walton: Appl. Phys. A **77**, 113 (2003)
11 Y.C. Choi, W.S. Kim, Y.S. Park, S.M. Lee, D.J. Bae, Y.H. Lee, G.S. Park, W.B. Choi, N.S. Lee, J.M. Kim: Adv. Mater. **12**, 746 (2000)
12 G.-S. Park, W.-B. Choi, J.-M. Kim, Y.C. Choi, Y.H. Lee, C.-B. Lim: J. Cryst. Growth **220**, 494 (2000)
13 H.Z. Zhang, Y.C. Kong, Y.Z. Wang, X. Du, Z.G. Bai, J.J. Wang, D.P. Yu, Y. Ding, Q.L. Hang, S.Q. Feng: Solid State Commun. **109**, 677 (1999)
14 B.C. Kim, K.T. Sun, K.S. Park, K.J. Im, T. Noh, M.Y. Sung, S. Kim: Appl. Phys. Lett. **80**, 479 (2002)
15 C.H. Liang, G.W. Meng, G.Z. Wang, Y.W. Wang, L.D. Zhang, S.Y. Zhang: Appl. Phys. Lett. **89**, 3202 (2001)

16 X.C. Wu, W.H. Song, W.D. Huang, M.H. Pu, B. Zhao, Y.P. Sun, J.J. Du: Chem. Phys. Lett. **328**, 5 (2000)
17 G. Gundiah, A. Govindaraj, C.N.R. Rao: Chem. Phys. Lett. **351**, 189 (2002)
18 P. Guha, S. Chakrabarti, S. Chaudhuri: Physica E **28**, 81 (2004)
19 J. Zhang, F. Jiang: Chem. Phys. **289**, 243 (2003)
20 J. Zhang, L.D. Zhang: Solid State Commun. **122**, 493 (2002)
21 J.-S. Lee, K. Park, S. Nahm, S.-W. Kim, S. Kim: J. Cryst. Growth **244**, 287 (2002)
22 Z.R. Dai, Z.W. Pan, Z.L. Wang: J. Phys. Chem. B **106**, 902 (2002)
23 J. Zhang, F. Jiang, L.D. Zhang: Phys. Lett. A **322**, 363 (2004)
24 B.Y. Geng, L.D. Zhang, G.W. Meng, T. Xie, X.S. Peng, Y. Lin: J. Cryst. Growth **259**, 291 (2003)
25 X. Xiang, C.-B. Cao, Y.-J. Guo, H.-S. Zhu: Chem. Phys. Lett. **378**, 660 (2003)
26 H.J. Yuan, S.S. Xie, D.F. Liu, X.Q. Yan, Z.P. Zhou, L.J. Ci, J.X. Wang, Y. Gao, L. Song, L.F. Liu, W.Y. Zhou, G. Wang: J. Cryst. Growth **258**, 225 (2003)
27 L.F. Dong, J. Jiao, M. Coulter, L. Love: Chem. Phys. Lett. **376**, 653 (2003)
28 N. Sakulchaicharoen, D.E. Resasco: Chem. Phys. Lett. **377**, 377 (2003)
29 J. Park, H.-H. Choi, K. Siebein, R.K. Singh: J. Cryst. Growth **258**, 342 (2003)
30 Y.W. Wang, L.D. Zhang, C.H. Liang, G.Z. Wang, X.S. Peng: Chem. Phys. Lett. **357**, 314 (2002)
31 X.B. Zeng, Y.Y. Xu, S.B. Zhang, Z.H. Hu, H.W. Diao, Y.Q. Wang, G.L. Kong, X.B. Liao: J. Cryst. Growth **247**, 13 (2003)
32 Z.Q. Liu, Z.W. Pan, L.F. Sun, D.S. Tang, W.Y. Zhou, G. Wang, L.X. Qian, S.S. Xie: J. Phys. Chem. Solids **61**, 1171 (2000)
33 T.Y. Kim, S.H. Lee, Y.H. Mo, H.W. Shim, K.S. Nahm, E.-K. Suh, J.W. Yang, K.Y. Lim, G.S. Park: J. Cryst. Growth **257**, 97 (2003)
34 S.S. Fan, J. Cao, H.Y. Dang, Q. Gu, J.H. Zhao: Mater. Sci. Eng. C **15**, 295 (2001)
35 I.Z. Rahman, K.M. Razeeb, M.A. Rahman, Md. Kamruzzaman: J. Magn. Magn. Mater. **262**, 166 (2003)
36 T. Harwig, F. Kellendouk: J. Solid State Chem. **24**, 25 (1978)
37 V.I. Vasil'tsiv, Y.M. Zakharko, Y.I. Prim: Ukr. Fiz. Zh. **33**, 1320 (1988)
38 L. Binet, D. Gourier: J. Phys. Chem. Solids **59**, 1241 (1998)
39 Y.P. Song, H.Z. Zhang, C. Lin, Y.W. Zhu, G.H. Li, F.H. Yang, D.P. Yu: Phys. Rev. B **69**, 075 304 (2004)